

Adaptive Laser Range Scanning

David MacKinnon, Victor Aitken, and François Blais

Abstract—We present an approach to laser range scanning in which quality metrics are used to automatically reduce the number of measurements acquired from a scanner viewpoint. As part of this approach we present improved versions of the orientation and reflectivity quality metrics, as well as introduce two quality metrics: resolvability and planarity. These quality metrics are used to divide the total field of view from a scanner viewpoint into regions. A subset of these regions is then automatically identified as having a significant likelihood of producing useful measurements to augment the initial range image using quality metrics. A series of targeted raster scans is then automatically generated to scan the targeted regions.

Index Terms—adaptive scanning, quality metrics, range imaging, automated scanning

I. INTRODUCTION

Currently absent in the field of medium-volume (1 to 10 metres) scanning is an interactive system capable of automatically obtaining a complete high-quality model of a scene or object *in situ* using an automated system, or by guiding a minimally-trained operator through the scanning process [1], while minimizing the number of measurements acquired. Some attempts have been made, most notably the work of Sequeira *et al.* [2], Blais *et al.* [3], and Callieri *et al.* [4]. Sequeira *et al.* used *quality metrics* for merging range images and, to a limited extent, for view planning. Blais *et al.* iteratively merged multiple low-density scans until a stable model was achieved. Callieri *et al.* used a multi-stage approach, first developed by Scott *et al.* [5] for small-volume scanning, in which an initial low-density scan is followed by a series of high-density targeted scans. In this paper, we present the first two stages of a multi-stage approach in which a series of quality metrics are used to adapt the scanning process such that the total quality of the final range image is maximized while minimizing the number of measurements acquired. Unlike Callieri *et al.*, this approach uses the strengths of each quality metric, allowing the scanning process to be better tailored to the surface being scanned.

The approach presented here is useful for situations in which visual quality of the resulting 3D model and cost of data acquisition is more critical than model precision. Examples are generating models for 3D displays or for CAD applications. In these cases, model acquisition costs can be minimized through the use of less well-trained operators and reduced scanning time, resulting in a visually acceptable 3D model. Specifically, the quality of the final model assumes

the anchor scan sampling density is sufficient to draw conclusions about the surface so missing the occasional small surface feature is an acceptable trade-off for reducing the cost of data acquisition.

II. QUALITY METRICS

The quality of a range measurement depends on measurement uncertainty and measurement resolution; however, spatial uncertainty is also strongly affected by other environmental factors such as the type of surface material [6], surface reflectivity [7], distance to the surface [7] [8], and incidence angle [9]. These environmental conditions must be detected in the data and combined with model-based uncertainty as metrics that further describe the quality of the virtual model. Few quality metrics exist in contemporary literature, and those that do are limited in scope. They are often not used in conjunction with the physical properties and limitations of the scanner and/or surface. In this paper a low-density raster scan is used to perform a cursory examination of the environment, then various environmental factors are quantified using general-purpose quality metrics that relate to the physical properties of the scanner. These metrics are then used to both determine the quality of the measurements collected, and to direct the scanning process such that the potential quality of the resulting composite range image is maximized with respect to the scanner limits while minimizing total scan time. Figure 1 shows the surface used in this paper to illustrate the process.



Fig. 1. Target object used to illustrate the adaptive scanning technique

The purpose of a quality metric is two-fold: it quantifies the relative position of some aspect of a range measurement on a continuum and it quantifies the relationship of that aspect of a range measurement to some previously established benchmark. A quality metric can then be used to either

D. MacKinnon and V. Aitken are with the Department of Systems and Computer Engineering, Carleton University, Ottawa, ON, Canada, K1S 5B6

F. Blais is with the Institute for Information Technology, National Research Council of Canada, Ottawa, ON, Canada, K1A 0R6

compare methods or systems or it can be used in an iterative process to maximize some aspect of a range image [10]. Two important components of a referenced quality metric are a clearly-defined *quality benchmark* against which to compare the current state of the range image, and a *quality scale* to indicate the degree to which the range measurement quality attribute deviates from the benchmark. The benchmarks are used to define the end points of the quality scale representing the best quality (1) and worst quality (0) associated with some attribute and must be attainable, or nearly attainable, by the system. The best quality benchmark represents the attribute state which is most desired by the system so represents a *target state*. The worst-quality benchmark represents an unacceptable state so represents a *breakpoint state*.

III. REGION-BASED ADAPTIVE SCANNING

Region-based adaptive scanning consists of extracting the regions of the total field of view (TFoV) that correspond to the surface of interest, then scanning only those regions likely to contribute useful and non-redundant information to the model of the object being scanned. An anchor scan is performed to initialize the region map. The region map is then analyzed to identify the portions that require rescanning to improve the quality of the final 3D model and which portions are likely to yield either redundant or unacceptable measurements. If the flagged regions occupy only a fraction of the region map then the total number of measurements acquired can be significantly reduced, resulting in a decrease in total scan time.

A. Anchor scan positioning

It is important that the viewpoint from which the anchor scan is obtained be close enough to the object to maximize the quality of each measurement while ensuring that as much of the object as possible is within the TFoV. The anchor scan could be used to select the next best view so it should contain as much information as possible about the object. On the other hand, the anchor scan should be obtained quickly and in a fashion that is amenable to automating the process of selecting the anchor scan viewpoint. Finally, the anchor scan should provide as many high-quality measurements as possible to the final 3D model. We achieve these goals by performing a series of pre-anchor scans using the weighted size of the laser spot. The size of the laser spot is weighted by the measurement orientation and resolvability quality metrics. A gradient search is then performed after each pre-anchor scan to predict a position and orientation for the scanner origin that is likely to reduce the *average weighted laser spot size* W_i^{spot} . This search space is restricted by the scanner geometry.

The optimal scanner position and orientation is approximated by minimizing the average weighted spot size. The weighted spot size of each measurement W_i^{spot} is defined by

$$W_i^{spot} = w(\zeta_i)(1 - C_i^{orient}C_i^{res}) \quad (1)$$

where $w(\zeta_i)$ is the radius of the laser spot assuming the surface normal is oriented along the laser path, ζ_i is the

distance from the surface to the beam waist, $C_i^{orient} \in [0, 1]$ is the orientation quality metric and $C_i^{res} \in [0, 1]$ is the resolvability quality metric. When C_i^{res} and C_i^{orient} are maximized then $W_i^{spot} = 0$ [11] [12]. The volume bounded by $w(\zeta_i)$ represents the region within which 86.5% of the beam irradiance is contained [13]–[15]. The average of the weighted spot sizes of all measurements is only calculated for measurements for which $C_i^{orient} > 0$ so that surfaces with normals oriented far from the laser path will be ignored.

The *orientation quality metric* C_i^{orient} is found using

$$C_i^{orient} = \begin{cases} 0 & c\gamma_i \leq c\gamma_{max} \\ \frac{c\gamma_i - c\gamma_{max}}{1 - c\gamma_{max}} & \text{otherwise} \end{cases} \quad (2)$$

where $c\gamma_i = \cos(\gamma_i)$ is the orientation of the surface at the point \mathbf{p}_i , and $c\gamma_{max} = \cos(\gamma_{max})$ which is the user-defined maximum acceptability [11] [12] [16]. Surface orientation is a commonly-used quality metric [17]–[22] and surfaces with high orientation are generally discarded during post processing because they result in low-quality measurements. Unlike contemporary orientation quality metrics, (2) generates a quality metric bounded by the target value $\cos(\gamma_i) = 1$ and the breakpoint $\cos(\gamma_i) = \cos(\gamma_{max})$. Measurements with $C_i^{orient} = 0$ arise from surfaces that are too highly angled so rescanning would yield measurements that would typically be discarded in post processing.

The resolvability quality metric C_i^{res} is used to identify regions that cannot be resolved at the desired surface resolution Δx given the current scanner viewpoint. This metric is found by

$$C_i^{res} = \begin{cases} 1 & d_i^{length} \leq d_i^{up} \\ \frac{d_i^{up} - d_i^{width}}{d_i^{length} - d_i^{width}} & d_i^{width} < d_i^{up} < d_i^{length} \\ 0 & d_i^{up} \leq d_i^{width} \end{cases} \quad (3)$$

where d_i^{length} is the length of the long axis of the beam footprint, d_i^{width} is the length of the short axis, and $d_i^{up} = \Delta x + 2d_i^{err}$ is the desired surface resolution with an error margin based on the measurement rotational uncertainty. The components of the long axis length are found using

$$\{d_i^{min}, d_i^{max}\} = \left| \frac{-K_{i,2} \pm \sqrt{K_{i,2}^2 - 4K_{i,1}K_{i,3}}}{2K_{i,1}} \right| \quad (4)$$

where

$$\begin{aligned} K_{i,1} &= [w(0) \sin(\gamma_i)]^2 - [\zeta_0 \cos(\gamma_i)]^2 \\ K_{i,2} &= 2\zeta_i w^2(0) \sin(\gamma_i) \\ K_{i,3} &= [w(0)\zeta_0]^2 + [w(0)\zeta_i]^2 \end{aligned} \quad (5)$$

while the d_i^{err} is based on the uncertainty in the position of the edge of the laser spot [11] [12].

The resolvability quality metric represents the smallest resolvable feature size but the sampling density of the subs cans takes into account the uncertainty in the rotational distance between any two neighbouring measurements. In order to ensure that the scanner is close enough to resolve

features to at least Δx with a margin of error, the error term d_i^{err} is added to the radial distance from the centre to the edge of the beam footprint. This error term is found using

$$d_i^{err} = \frac{R \sin(\theta_{err})}{\cos(\gamma_i) - \sin(\gamma_i) \sin(\theta_{err})} \quad (6)$$

where γ_i is the angle between the surface normal and the laser path. The rotational error term θ_{err} is defined as

$$\theta_{err} = \sqrt{\chi^2(1, \alpha) (\max\{\sigma_\theta^2, \sigma_\phi^2\})} \quad (7)$$

where $\chi^2(1, \alpha) \approx 3.84$ for $\alpha = 0.05$, and σ_θ and σ_ϕ are the horizontal (θ) and vertical (ϕ) rotational uncertainties. The θ_{err} term represents the maximum distance between two points, in this case the centre of one beam footprint and the edge of its neighbouring beam footprint, such that they can still be considered likely to represent the same point to within a 95% confidence level given the expected rotational uncertainty of the scanner.

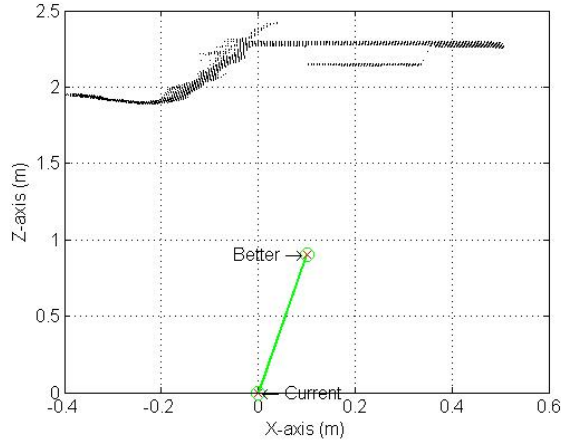


Fig. 2. First recommended scanner motion to improve average weighted spot size quality

Figure 2 illustrates the results of using the average weighted spot size minimization (AWSM) method and corresponds to the first row of Table I. The weighted spot size of each measurement in the pre-anchor scan was calculated using (1), then a gradient search was performed by virtually moving the scanner viewpoint in a direction that maximizes the decrease in the average weighted spot size to within the limits of the search space. The search terminated when moving the scanner in any direction would result in no further weighted spot size reduction. The scanner could only be moved horizontally (along the z-axis) and laterally (along the x-axis), and scanner positions closer than 0.5 metres to the surface were excluded from the search space to avoid collision between the scanner and the surface. The target surface resolution for the resolvability quality metric was defined to be $\Delta x = 2$ millimetres. After three iterations, a local quality maxima was reached in which further adjustment of the scanner viewpoint was predicted to result in no reduction in quality-weighted spot size.

TABLE I

W^{spot} REDUCTION THROUGH ITERATIVE SCANNER PLACEMENT

Initial W^{spot}	Predicted W^{spot}	Requested Translation (m)	Requested Rotation
7.305	0.586	X=0.1/ Y=0/ Z=0.9	$\theta=4^\circ$ / $\phi=11^\circ$
0.327	0.277	X=0.0/ Y=0/ Z=-0.1	$\theta=-1^\circ$ / $\phi=2^\circ$
0.332	0.332	X=0.0/ Y=0/ Z=0.0	$\theta=-1^\circ$ / $\phi=2^\circ$

B. Region Classification

Once the anchor range image has been acquired, the region map is initialized by classifying regions as either *Complete*, *Unscannable*, or *Rescan*. Not all measurements in a range image yield usable data; in some cases, the return signal is either insufficient to be detected (*drop-out measurement*) or exceeds the capacity of the photodetector (*saturated measurement*). In either case, the spatial and intensity measurement cannot be obtained so is generally assigned a value of zero. These measurements are referred to here as *non-return measurements*, while measurements that generate a non-zero range and intensity value are defined as *return measurements*. A Delaunay facet map of the horizontal (θ) and vertical (ϕ) rotation measurements is generated for all measurements, then all facets for which all vertices are non-return measurements are classified as being part of the Unscannable region. Similarly, all facets for which all vertices are return measurements are classified as being part of the Complete region. Non-return measurements are often discarded; however, the presence of non-return measurements indicates the transition between a Complete region and an Unscannable region. All facets not already classified as Unscannable or Complete are classified as being part of the Rescan region.

High-density scanning of the Unscannable region would yield few, if any, non-zero measurements so measurements from within this region are not flagged for rescanning. Facets composed of a mix of return and non-return vertices define the Rescan region, which will contain *mixed measurements* [7] [23]–[25]. The Rescan region must be scanned at high density so that the point of transition between return and non-return measurements can be isolated in the composite range image. What remains is to move any areas of the the Complete region that should be rescanned to the Rescan region, and to move any areas of the Complete region that, if rescanned, would contribute little to the final 3D model to the Unscannable region.

C. Planarity Detection

The first step in identifying areas requiring high-density scans within the Complete region is to identify portions of the Complete region containing spatially complex surfaces. A spatially complex surface results in range measurements that change rapidly within the resolution of the system and require sampling at the maximum density of the scanning system to ensure that they are accurately represented in the final 3D model. The Complete region is examined to identify

which subregions are unlikely to contain spatial complexity. Areas of the Complete region that have not been identified as being spatially non-complex are then moved to the Rescan region so that the Complete region consists only of spatially non-complex areas. For the purpose of identifying spatially non-complex areas, measurements arising from locally planar neighbourhoods are classified as *planar measurements*, using Stamos and Allen's method for planar segmentation [26]. The neighbourhood of a measurement \mathbf{p}_i is defined as the set of all 8 measurements that surround \mathbf{p}_i in the raster scan, what is referred to as an *8-neighbourhood* [27].

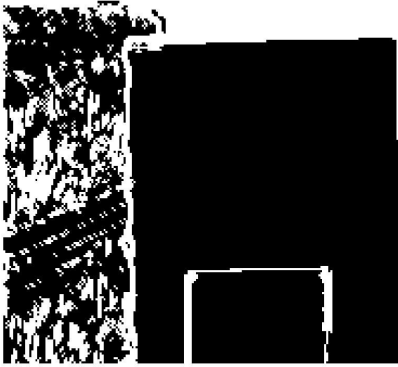


Fig. 3. Complete region map after spatial complexity analysis in which black areas represent the Complete region

Planarity as a quality metric has not been defined in current literature, yet measurements arising from planar surfaces, assuming all other attributes are near ideal, are of high quality because they are unlikely to contain surface discontinuities that can introduce range errors. The *planarity quality metric* C_i^{planar} is defined to represent the deviation of the neighbourhood of a measurement from the assumption of being a planar surface. Planarity is a *binary quality metric*; a measurement is either part of a planar neighbourhood ($C_i^{planar} = 1$) or it is not ($C_i^{planar} = 0$). Figure 3 shows the Complete region map for the anchor scan which initially consists only of measurements arising from planar neighbourhoods. If the anchor scan measurements are reasonably indicative of the surface geometry, then performing high-density scans of areas consisting of planar neighbourhoods should add little new information to the range model. Facets in which all vertices have $C_i^{planar} = 1$ are classified as being part of the Complete region and are initially excluded from the rescan list.

D. Reflectivity Transitions

Changes in surface reflectivity can be used to identify potential range or reflectivity discontinuities. A reduction in surface reflectivity can increase measurement uncertainty [7] so any deviation from the reference represents a potential change in real measurement uncertainty from that predicted by the model. The *reflectivity quality metric* $C_i^{reflect}$ is

defined to be

$$C_i^{reflect} = \begin{cases} 0 & \rho_i \geq \rho_{max} \\ \frac{\rho_{max} - \rho_i}{\rho_{max} - 1} & \rho_{max} > \rho_i > 1 \\ 1 & \rho_i = 1 \\ \frac{\rho_i - \rho_{min}}{1 - \rho_{min}} & \rho_{min} < \rho_i < 1 \\ 0 & \rho_i \leq \rho_{min} \end{cases} \quad (8)$$

where ρ_{min} and ρ_{max} are user-defined bounds on the acceptable reflectivity of the surface, and ρ_i is the surface reflectivity relative to a reference surface [11] [12] [16]. Fiocco *et. al.* [22] had previously defined a reflectivity quality metric as a binary quality metric; however, their approach reduces the generalizability of the metric.

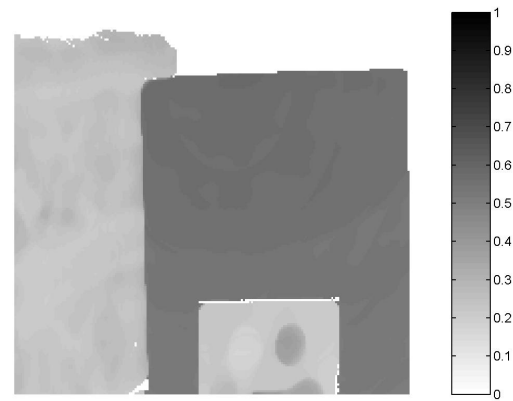


Fig. 4. Reflectivity Quality Map in which dark regions represent high-quality measurements (similar to reference level) and light regions represent low-quality measurements (different from reference level)

The picture of four distributor caps, visible in Figure 1, appears as a flat plane in Figure 3, but the transitions between high (dark regions) and low (light regions) reflectivity areas within the picture are visible in the Reflectivity Quality Map in Figure 4 and can generate range errors. Sobel edge detection was performed for each 8-neighbourhood by marking the measurement as an edge if the reflectivity difference between the measurement and any of its neighbours exceeded an experimentally-determined threshold level $\Delta C_i^{reflect} = 0.1$. Areas of the Complete region containing measurements marked as being a reflectivity edge are moved to the Rescan region are included in the rescan list. Figure 5 shows the effect on the Complete region map of moving areas with Reflectivity quality metric edges to the Rescan region.

E. Orientation and Resolvability

All facets in the region map in which at least one vertex has $C_i^{resolve} = 0$ are classified as *Unresolvable* and are merged into the Unscannable region. Similarly, facets in the region map for which any vertex had $C_i^{orient} = 0$ are classified as *Angled* and are also merged into the Unscannable region. Highly angled surfaces are typically removed during post-processing; however, removing them as part of the

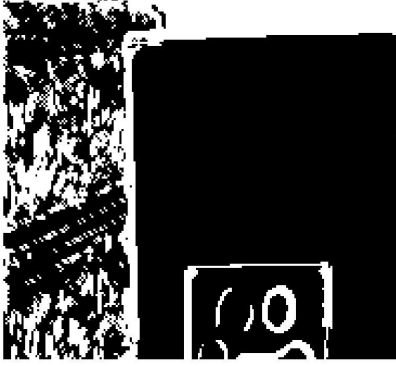


Fig. 5. Complete region map after transitions in the reflectivity quality metric have been included have been moved to the Rescan region

data collection process reduces the number of measurements obtained that would normally be discarded.

After all region assignment has been completed, rescanning is restricted to only the Rescan regions. As a result, the number of high-density scans required to generate the composite range image can be significantly reduced. Figure 6 shows the final Region Map in which Rescan regions are in dark grey, and Complete regions are in light grey.

IV. SUBSCAN GENERATION

A series of raster subs cans are generated to acquire high-density range information only from the Rescan region. The Rescan region is initially bounded by a box representing the total rotational coverage without overlap while ensuring that the surface can be sampled to at least the target resolution Δx after taking surface orientation and rotational uncertainty into account. The bounding box is first divided into subs cans, then any subs cans that do not cover a Rescan region are removed. The subs cans are then shifted to maximize Rescan region coverage while minimizing coverage of the Unscannable region. This generally results in a further reduction in the number of subs cans performed. Figure 6 shows the first stage subs can map for the object shown in Figure 1. Solid boxes represent the effective scanning region while the dashed boxes represent the area covered by the raster scan.

The coverage of each subs can is examined to ensure that the Rescan region has been completely scanned at high density and to ensure that no aliasing is detected. If portions of the Rescan region have not been covered by subs cans then the overlap among subs cans is automatically increased for all future subs cans, and the unscanned portions the Rescan region are rescanned. The coverage of each subs can is also examined to ensure that no aliasing is detected. If Aliased measurements are detected in the subs cans then the sampling density is automatically increased for all future subs cans to minimize the chance of Aliased measurements being generated. The Aliased and unscanned portions of the Region Map are rescanned as Stage 2 subs cans.

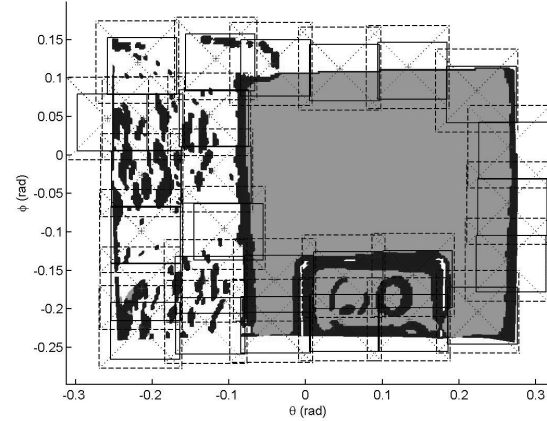


Fig. 6. Final Region Map with first stage subs cans. The Unscannable region is in white, the Rescan region is in dark grey, and the Planar region is in light grey. Each box represents a single subs can.

TABLE II

SCANNER EFFICIENCY VERSUS TFOV SCAN TIME OF 118.9 MINUTES

Anchor scans	3
Stage 1 subs cans	27
Stage 2 subs cans	85
Data Processing (min)	28.56
Scanning Time (min)	20.24
Total (min)	53.28
Fraction of TFOV Scan	0.410

A total of 112 subs cans are required to sample the surface at sufficient density to resolve features to at least 2 millimetres after taking into account rotational uncertainty. Table II shows the time required for both data processing and scanning. Data processing was performed using Matlab 7.0 on a 3.0 GHz Pentium processing running Windows XP. Time required to move the scanner between pre-anchor scans and time to transfer data from the scanner workstation to the processing workstation were not included in the total. The total time required to obtain and process the scans was 41.0% of the time it would have taken to simply scan the total field of view at the same sampling resolution (118.9 minutes).

V. CONCLUSIONS

An intelligent application of spot size, planarity, orientation, reflectivity and resolvability quality metrics can be used to significantly reduce the number of regions scanned at high resolution, resulting in a significant reduction in total time spent scanning the surface. The AWSM method is used to automatically minimize laser spot size while ensuring that surface features can be resolved to at least the desired sampling resolution. Planarity, orientation, reflectivity and resolvability quality metrics are then used to automatically generate a list of regions within the total field of view that should be rescanned at high resolution. The multi-stage scanning approach presented here can be used in both fully

automated scanning systems as well as systems that guide a minimally trained operator.

VI. FUTURE WORK

Future work will examine how these and other quality metrics can be used to perform view planning to achieve the desired sampling density. Additional work is also required to generate subsfans such that the number of non-return and discarded measurements is minimized using non-raster patterns. Finally, future work will also explore using quality-based methods for merging composite range images obtained from different viewpoints.

VII. ACKNOWLEDGMENTS

We would like to thank the National Research Council of Canada for providing funding for this research through the Graduate Student Scholarship Supplement, as well as for providing facilities and equipment. We would, in particular, like to thank Michel Picard and Luc Cournoyer for assistance with setup and operation of the laser range scanner used in this study.

REFERENCES

- [1] L. Van Gool, B. Leibe, P. Muller, M. Vergauwen, and T. Weise, "3D Challenges and a Non-In-Depth Overview of Recent Progress," in *Proceedings of the Sixth International Conference on 3-D Digital Imaging and Modeling*, G. Godin, P. Hebert, T. Masuda, and G. Taubin, Eds., Montréal, Québec, CAN, 21-23 August 2007, pp. 118–129.
- [2] V. Sequeira, K. Ng, E. Wolfart, J. G. M. Goncalves, and D. Hogg, "Automated reconstruction of 3D models from real environments," *ISPRS Journal of Photogrammetry and Remote Sensing*, vol. 54, no. 1, pp. 1–22, February 1999.
- [3] F. Blais, M. Picard, and G. Godin, "Recursive Model Optimization Using ICP and Free Moving 3D Data Acquisition," in *Proceedings of the 4th International Conference on 3-D Digital Imaging and Modeling*, Banff, ALB, Canada, 6–10 October 2003.
- [4] M. Callieri, A. Fasano, G. Impoco, P. Cignoni, R. Scopigno, G. Parrini, and G. Biagini, "RoboScan: an automatic system for accurate and unattended 3D scanning," in *Proceedings of the 2nd International Symposium on 3D Data Processing, Visualization and Transmission*, 6-9 September 2004, pp. 805–812.
- [5] W. Scott, G. Roth, and J.-F. Rivest, "View Planning for Multi-Stage Object Reconstruction," in *Proceedings of Vision Interface*, Ottawa, ON, Canada, June 2001, pp. 64–71.
- [6] M. Adams, "Lidar design, use, and calibration concepts for correct environmental detection," *IEEE Transactions on Robotics and Automation*, vol. 16, no. 6, pp. 753–761, December 2000.
- [7] J. Hancock, D. Langer, M. Hebert, R. Sullivan, D. Ingimarsen, E. Hoffman, M. Mettenleiter, and C. Froehlich, "Active laser radar for high-performance measurements," in *Proceedings of the IEEE International Conference on Robotics and Automation*, vol. 2, Leuven, Belgium, 16-20 May 1998, pp. 1465–1470.
- [8] J.-A. Beraldin, M. Picard, S. El-Hakim, G. Godin, L. Borgeat, F. Blais, E. Paquet, M. Rioux, V. Valzano, and A. Bandiera, "Virtual Reconstruction of Heritage Sites: Opportunities and Challenges Created by 3D Technologies," in *Proceedings of the International Workshop on Recording, Modeling and Visualization of Cultural Heritage*, Ascona, Switzerland, 22-27 May 2005.
- [9] A. Johnson, R. Hoffman, J. Osborn, and M. Hebert, "A system for semi-automatic modeling of complex environments," in *Proceedings of the International Conference on Recent Advances in 3-D Digital Imaging and Modeling*, Ottawa, ON, Canada, 12–15 May 1997, pp. 213–220.
- [10] W. Scott, G. Roth, and J. Rivest, "Performance-Oriented View Planning for Model Acquisition," in *Proceedings of the The International Symposium on Robotics*, Montréal, QUE, Canada, May 2000, pp. 212–219.
- [11] D. MacKinnon, V. Aitken, and F. Blais, "Using Quality Metrics with Laser Range Scanners," in *Proceedings of the IST&T/SPIE 20th Annual Symposium on Electronic Imaging Science and Technology*, San Jose, CA, USA, 27–31 January 2008.
- [12] —, "Adaptive Laser Range Scanning using Quality Metrics," in *Proceedings of the IEEE International Instrumentation and Measurement Technology Conference*, Victoria, BC, CAN, 12–15 May 2008.
- [13] B. Chu, *Laser Light Scattering Basic Principles and Practice*, 2nd ed. Academic Press, Inc., 1991, pp. 156–160.
- [14] G. Jacobs, "Understanding Spot Size for Laser Scanning," *Professional Surveyor Magazine*, October 2006.
- [15] D. Williams, *Optical Methods in Engineering Metrology*, 1st ed. Chapman & Hall, 1993, pp. 11–16.
- [16] D. MacKinnon, V. Aitken, F. Blais, and M. Picard, "Adaptive Laser Range Scanning," in *Proceedings of the IEEE International Workshop on Robotic and Sensors Environments*, Ottawa, ON, Canada, 12–13 October 2007.
- [17] V. Sequeira, K. Ng, E. Wolfart, J. G. Goncalves, and D. Hogg, "Automated 3D reconstruction of interiors with multiple scan-views," in *Proceedings of SPIE*, vol. 3641, 1998, pp. 106–117.
- [18] B. L. Curless, "New methods for surface reconstruction from range images," PhD Thesis, Stanford University, 1997.
- [19] M. Rutishauser, M. Stricker, and M. Trobina, "Merging range images of arbitrarily shaped objects," in *Proceedings of the IEEE Computer Society Conference on Computer Vision and Pattern Recognition*, 21–23 June 1994, pp. 573–580.
- [20] M. Soucy, A. Croteau, and D. Laurendeau, "A multi-resolution surface model for compact representation of range images," in *Proceedings of the IEEE International Conference on Robotics and Automation*, vol. 2, Nice, France, 12–14 May 1992, pp. 1701–1706.
- [21] G. Turk and M. Levoy, "Zippered Polygon Meshes from Range Images," in *SIGGRAPH-94*, 1994, pp. 311–318.
- [22] M. Fiocco, G. Boström, J. Gonçalves, and V. Sequeira, "Multisensor fusion for Volumetric Reconstruction of Large Outdoor Areas," in *Proceedings of the Fifth International Conference on 3-D Digital Imaging and Modeling*, 2005.
- [23] W. R. Scott, G. Roth, and J.-F. Rivest, "View planning for automated three-dimensional object reconstruction and inspection," *ACM Computing Surveys*, vol. 35, no. 1, pp. 64–96, March 2003.
- [24] M. Hebert and E. Krotkov, "3-D measurements from imaging laser radars: how good are they?" in *Proceedings of the IEEE/RSJ International Workshop on Intelligent Robots and Systems*, vol. 1, 3–5 November 1991, pp. 359–364.
- [25] J. Tuley, N. Vandapel, and M. Hebert, "Analysis and Removal of artifacts in 3-D LADAR Data," in *Proceedings of the IEEE International Conference on Robotics and Automation*. IEEE, January 2005.
- [26] I. Stamos and P. K. Allen, "3-D Model Construction Using Range and Image Data," in *Proceedings of the IEEE Conference on Computer Vision and Pattern Recognition*, vol. 1, Hilton Head Island, SC, USA, 13–15 June 2000, pp. 531–536.
- [27] V. Lacroix and M. Acheroy, "Feature extraction using the constrained gradient," *ISPRS Journal of Photogrammetry and Remote Sensing*, vol. 53, no. 2, pp. 85–94, April 1998.